EXPERIMENTAL INVESTIGATION OF CRACK OPENING ASYMPTOTICS FOR FLUID-DRIVEN FRACTURE

Andrew P. Bunger[1], Robert G. Jeffrey[1] and Emmanuel Detournay[2]
[1] CSIRO Division of Petroleum Resources, Melbourne, Australia
[2] Department of Civil Engineering, University of Minnesota, Minneapolis, MN 55455 USA

ABSTRACT

The tip region of a fluid-driven fracture is governed not only by the square-root tip asymptote, well-known from linear elastic fracture mechanics (LEFM), but also by an intermediate asymptotic solution which comprises a tip asymptote specific to fluid-driven fracture. These tip asymptotics were explored in the laboratory by growing hydraulic fractures in impermeable, transparent, brittle elastic materials, employing a method based on the Beer-Lambert law of optical absorption to measure the full-field fracture opening from the intensity of light transmitted through the growing fractures. It was found that a power-law of the distance from the crack tip fit the opening data well over the outer 30 to 40 percent of the fracture. This power law was found to approximately match the fluid-driven fracture tip asymptote when the effect of fluid viscosity, quantified by a dimensionless parameter, was significant. Conversely, the LEFM tip asymptote approximated the experimental behavior when the effect of viscosity was negligible. These results give the first direct experimental evidence for the existence of the fluid-driven fracture tip solution. However, the implications will be fully understood only when solutions are developed which consider more general cases, specifically in the case with large fluid lag and the case of a fracture parallel to a nearby free surface.

1 INTRODUCTION

This paper presents experimental results regarding the nature of crack-tip asymptotics for a fluid-driven fracture in an impermeable elastic medium. Linear elastic fracture mechanics (LEFM) gives the following asymptotic form for crack-tip opening (Rice [1])

$$w \sim 4\left(\frac{2}{\pi}\right)^{1/2}\frac{K_{Ic}}{E'}x^{1/2}, \qquad \frac{x}{R} \ll 1, \tag{1}$$

where K_{Ic} is the fracture toughness, E' is the plane strain modulus, x is the distance from the crack tip, and R is the fracture radius (or half-length). However, when the fracture is driven by a power-law fluid, the coupling between linear elasticity and lubrication theory leads under certain conditions to an intermediate asymptotic tip solution which is peculiar to hydraulic fracture (Desroches *et al.* [2], Garagash and Detournay [3]). For the simplest case of a Newtonian fluid with viscosity μ, this asymptotic form is given by

$$w \sim 2\, 3^{7/6}\left(\frac{\mu}{E'}\right)^{1/3}\left(\frac{dR_f}{dt}\right)^{1/3}x^{2/3}, \qquad \frac{x}{R} \ll 1, \tag{2}$$

where R_f is the radius of the fluid-filled region. This is a modification of published analyses, which assume that the size of the fluid lag - the region between the fluid-filled region and fracture front - is negligible ($R_f/R \approx 1$). This asymptotic behavior is a direct consequence of the mathematical model, a fact that was reported even before it was specifically attributed to an intermediate asymptotic solution (Spence and Sharpe [4], Lister [5]). Furthermore, consideration of this crack-tip behavior is fundamental to a number of recent contributions (e.g.

Savitski and Detournay [6], Adachi [7]), however, to date there has been no experimental evidence to support it.

In the following we present experiments in which full-field fracture opening is measured and the data related to the asymptotic forms (eqns 1 and 2). Both asymptotes are observed and it is shown that dominance of one asymptote over the other is related to the value of a parameter which has the interpretation of a dimensionless viscosity.

2 CHARACTERISTIC TIMESCALES

Letting $\langle Q \rangle$ be the mean injection rate up to time t, it may be shown from scaling laws derived from the governing equations (linear elasticity, lubrication theory, and fluid volume balance) that the penny-shaped fracture in an impermeable elastic solid evolves in a single dimensionless parameter (Savitski and Detournay [6])

$$\mathcal{M} = \left(\frac{t_{mk}}{t} \right)^{2/5}, \qquad t_{mk} = \left(\frac{\mu^5 \langle Q \rangle^3 E'^{13}}{K_{Ic}^{18}} \right)^{1/2}, \tag{3}$$

which may be interpreted as a dimensionless viscosity. Hence, at early time the *effective* viscosity is significant, resulting in strong coupling between the fluid and solid mechanics. Along with this strong coupling comes the potential for large fluid pressure gradients to exist and the possibility of developing substantial fluid lag (Garagash [8]). The problem evolves relative to the characteristic time t_{mk} to a regime where the fluid/solid coupling becomes weak (toughness-dominated), and in the limit vanishes (zero-viscosity). Therefore at large time the pressure gradient and fluid lag vanish, as does the intermediate asymptotic solution (eqn 2).

Hydraulic fractures growing parallel to a nearby free-surface evolve on a second timescale related to the growth of the fracture length with respect to the fracture depth H. For the penny-shaped fracture this timescale is given by (Bunger and Detournay [9])

$$t_{k\bar{k}} = \frac{K_{Ic} H^{5/2}}{\langle Q \rangle E'}. \tag{4}$$

Thus near-surface hydraulic fracture in an impermeable solid evolves on two timescales, and in fact, it may be shown that the fracture is uniquely characterized by the ratio (Bunger and Detournay [10])

$$\bar{\mathcal{M}}_k = \frac{t_{mk}}{t_{k\bar{k}}} = \mu \frac{E'^3 \langle Q \rangle}{H K_{Ic}^4}. \tag{5}$$

Provided that the fractures grow only to some multiple of the depth that is of order one, timescale $t_{k\bar{k}}$ gives the order of magnitude of the time required for a particular fracture to grow. It follows directly that limiting regimes of fracture exist, for example, if $\bar{\mathcal{M}}_k \ll 1$, the fracture grows almost entirely in an essentially uncoupled regime where fluid viscosity plays no significant role (Detournay [11]).

3 EXPERIMENTAL METHOD

We have developed experiments to explore these regimes of fracture propagation. One series of tests, performed in Polymethylmethacrylate (PMMA) ($E' = 3900$ MPa, $K_{Ic} = 1.4$ MPa m$^{1/2}$), was designed such that $\bar{\mathcal{M}}_k \ll 1$. A second series, designed such that $\bar{\mathcal{M}}_k = O(1)$, was performed in borosilicate glass ($E' = 65000$ MPa, $K_{Ic} = 0.7$ MPa m$^{1/2}$). Fractures were

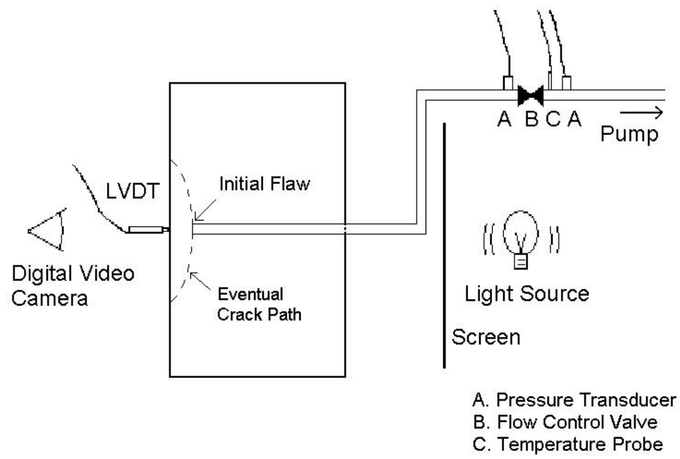

Figure 1: Sketch of experimental setup.

driven by aqueous glycerin, a Newtonian fluid with a viscosity which may be easily varied from 0.001 to 2.5 Pa·s depending on water content and temperature. Initiation occurred from a pre-existing manufactured flaw with initial radius of 10 mm and initial depth of 12 to 15 mm.

Injection fluids contained a proportion of aqueous blue dye, and a video camera recorded the intensity of light transmitted through the growing fracture from a back-light source (Figure 1). In this way, opening was determined from the optical absorbance A of the fluid-filled portion of the fracture according to the well-known Beer-Lambert law

$$A \equiv \log \frac{I_o}{I} = \frac{w}{k}, \tag{6}$$

where k is a constant determined by calibrating with fluid-filled wedges. Additionally, pressure was measured using analog transducers, injection rate was estimated from pressure drop across a needle-type flow control valve, surface displacement at the fracture center was measured using an linear variable differential transformer (LVDT), and fracture radius R and fluid radius R_f were determined directly from video images of the growing fracture.

4 ANALYSIS AND DISCUSSION

Intensity (grayscale) images were captured from the video of each test. An example is shown in Figure 2 for a case where fluid lag is easily observed. For each image, eqn (6) was used to compute the average value of the opening, sampled along 15-20 radial lines. The effect of the viscosity parameter on the crack tip opening is shown in Figure 3. In the first, small viscosity case, the opening follows closely with eqn (1). Conversely, in the second case eqn (2) closely approximates fracture opening.

The power-law model

$$w = C\xi^{\alpha}, \qquad \xi = \frac{x}{R}, \tag{7}$$

was fit to the data using a least-squares procedure. Generally, the identification of the coefficients C and α used the data over the approximate range $0.3 < \xi < R_f/R$; however

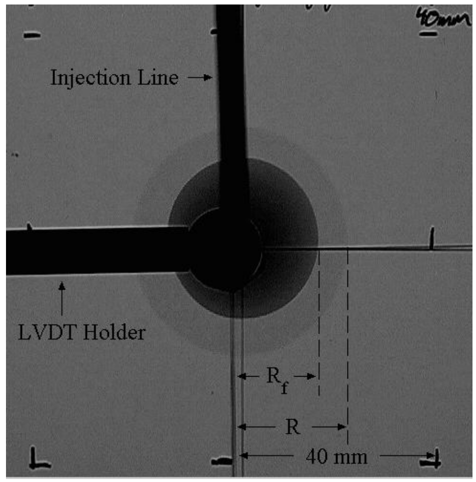

Figure 2: Image of growing hydraulic fracture, $H = 13$ mm, $\bar{\mathcal{M}}_k \approx 2$.

C and α do not appear to be sensitive to the exact choice of data range. Figure 4 shows two plots corresponding to each of two representative tests. The first plot shows the exponent α versus the fracture radius to depth ratio. The fluid fraction R_f/R, in the range $0.55 < R_f/R < 1$ for the second test, is also shown for reference. The second plot shows the intensity parameter computed from each experimental data point, C_{exp}. Plotted with these values are the intensity parameters from eqns (1) and (2), $C_{1/2}$ and $C_{2/3}$ respectively, which are computed using the material properties and the experimental data for R and R_f. Examination of Figure 4 along with plots like those in Figure 3 shows that the power law that is the best fit to the experimental data also coincides with the appropriate tip asymptote (eqn 1 or 2) within 10 to 20 percent throughout fracture propagation. There are two exceptions. At early time, the influence of the borehole on the stress field and/or the influence of fluid compressibility on the injection rate may play a significant role. The other exception occurs for fluid fraction R_f/R less than 0.7, in which case it is probable that there is insufficient overlap between the fluid-filled region and the tip region for eqn (2) to hold.

5 CONCLUSIONS

These results provide, to the authors' knowledge, the first direct experimental evidence supporting the existence of an intermediate asymptotic tip solution associated with the two-thirds asymptotic behavior. Furthermore, experimental evidence supports the assertion that this tip asymptote, a result of solid/fluid coupling, vanishes when the effect of the viscosity becomes small (Garagash [12]). However, the hydraulic fracture solutions (Desroches *et al.* [2], Garagash and Detournay [3]) which are shown here to agree with the experimental data, assume that the size of the fluid lag region is negligible relative to the crack length. Furthermore, tip asymptotics for near-surface hydraulic fracture are not yet fully understood. Thus it is not known what tip behavior the mathematical model predicts when there is significant fluid lag or when the fracture radius is large relative to the fracture depth, so the implications of these results will be fully understood only when appropriate solutions are developed.

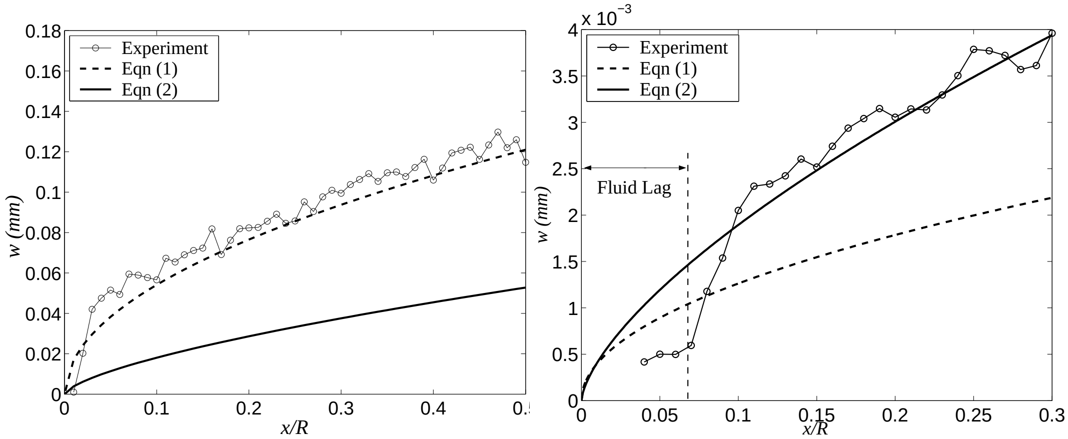

Figure 3: Fracture opening versus normalized distance from fracture tip for dimensionless viscosity parameter $\bar{\mathcal{M}}_k \approx 0.03$ (left) and $\bar{\mathcal{M}}_k \approx 0.7$ (right).

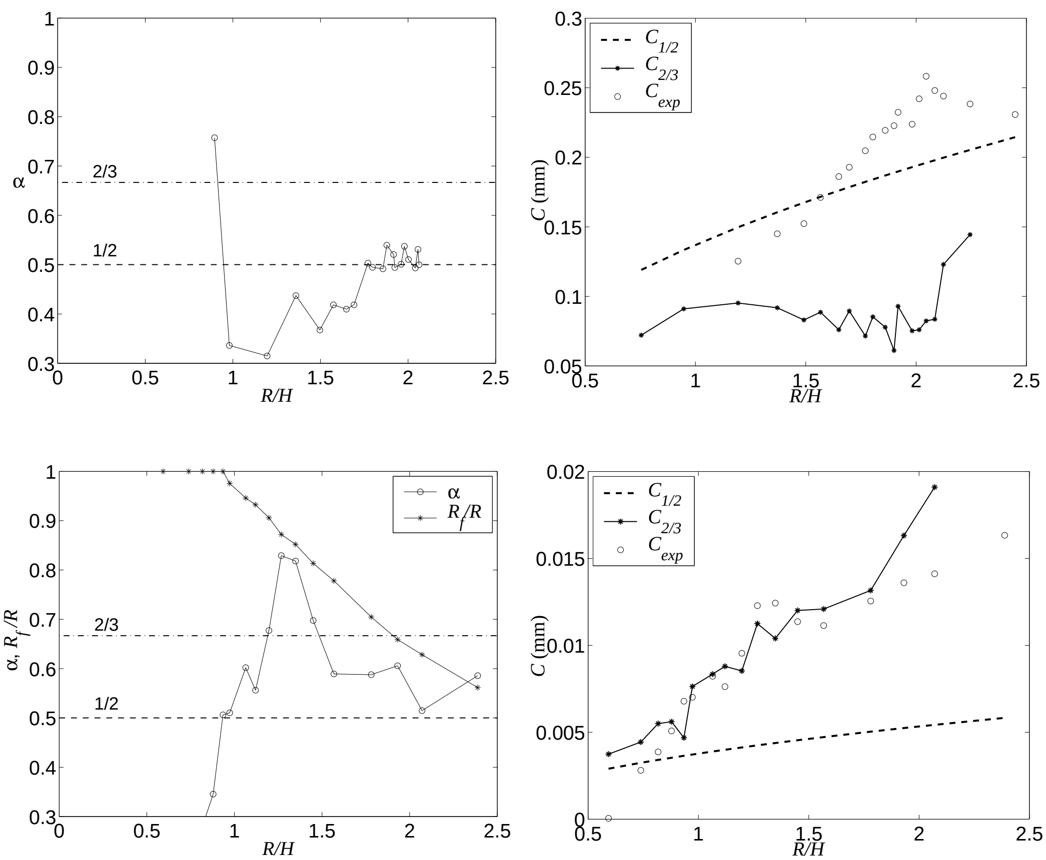

Figure 4: Results for power and intensity parameters from eqns 1 and 2 where $\bar{\mathcal{M}}_k \approx 0.03$ - no lag (top) and $\bar{\mathcal{M}}_k \approx 0.7$ (bottom).

ACKNOWLEDGMENT

The authors wish to acknowledge funding from the Australian Coal Association Research Program (ACARP). Additional support has been provided by CSIRO Petroleum, the Theodore Bennett Chair, and Schlumberger.

REFERENCES

[1] Rice, J.R. Mathematical analysis in the mechanics of fracture. In H. Liebowitz, editor, *Fracture, an Advanced Treatise*, volume II, chapter 3, pages 191–311. Academic Press, New York NY, 1968.

[2] Desroches, J., Detournay, E., Lenoach, B., Papanastasiou, P., Pearson, J.R.A., Thiercelin, M. and Cheng, A.H-D. The crack tip region in hydraulic fracturing. *Proc. Roy. Soc. London*, Series A(447):39–48, 1994.

[3] Garagash, D. I. and Detournay, E. The tip region of a fluid-driven fracture in an elastic medium. *ASME J. Appl. Mech.*, 67:183–192, 2000.

[4] Spence, D.A. and Sharp, P.W. Self-similar solution for elastohydrodynamic cavity flow. *Proc. Roy. Soc. London*, Series A(400):289–313, 1985.

[5] Lister, J.R. Buoyancy-driven fluid fracture: The effects of material toughness and of low-viscosity precursors. *J. Fluid Mech.*, 210:263–280, 1990.

[6] Savitski, A. and Detournay, E. Propagation of a penny-shaped fluid-driven fracture in an impermeable rock: asymptotic solutions. *Int. J. Solids Struct.*, 39:6311–6337, 2002.

[7] Adachi, J. *Fluid-Driven Fracture in Permeable Rock*. PhD thesis, University of Minnesota, Minneapolis, MN.

[8] Garagash, D. Hydraulic fracture propagation in elastic rock with large toughness. In J. Girard, M. Liebman, C. Breeds, and T. Doe, editors, *Rock Around the Rim – Proc. 4th North American Rock Mechanics Symposium*, pages 221–228, Rotterdam, 2000. Balkema.

[9] Bunger, A.P. and Detournay, E. Asymptotic solution for a penny-shaped near-surface hydraulic fracture. *Eng. Fract. Mec.*, 2004. To be submitted.

[10] Bunger, A.P. and Detournay, E. Scaling and intermediate asymptotic behavior of hydraulic fractures growing parallel to a free-surface. *SIAM*, 2004. To be submitted.

[11] Detournay, E. Propagation regimes of fluid-driven fractures in impermeable rocks. *Int. J. Geomechanics*, 4(1):1–11, 2004.

[12] Garagash, D. I. Influence of confining stress on plane-strain propagation of fluid-driven fracture I: Asymptotic regimes. *Int. J. Solids Struct.*, 2004. To be submitted.